6-2009

Temperature dependence of hot-carrier relaxation in PbSe nanocrystals: An ab initio study

Hua Bao
Purdue University - Main Campus

Bradley F. Habenicht
University of Washington - Seattle Campus

Oleg V. Prezhdo
University of Washington - Seattle Campus

X Ruan
Purdue University, ruan@purdue.edu

Temperature dependence of hot-carrier relaxation in PbSe nanocrystals: An *ab initio* study

Hua Bao,[1] Bradley F. Habenicht,[2] Oleg V. Prezhdo,[2,*,†] and Xiulin Ruan[1,*,‡]
[1]*School of Mechanical Engineering and The Birck Nanotechnology Center , Purdue University, West Lafayette, Indiana 47907, USA*
[2]*Department of Chemistry, University of Washington, Seattle, Washington 98195, USA*
(Received 19 February 2009; revised manuscript received 26 April 2009; published 3 June 2009)

Temperature-dependent dynamics of phonon-assisted relaxation of hot carriers, both electrons and holes, is studied in a PbSe nanocrystal using *ab initio* time-domain density-functional theory. The electronic structure is first calculated, showing that the hole states are denser than the electron states. Fourier transforms of the time-resolved energy levels show that the hot carriers couple to both acoustic and optical phonons. At higher temperature, more phonon modes in the high-frequency range participate in the relaxation process due to their increased occupation number. The phonon-assisted hot-carrier relaxation time is predicted using nonadiabatic molecular dynamics, and the results clearly show a temperature-activation behavior. The complex temperature dependence is attributed to the combined effects of the phonon occupation number and the thermal expansion. Comparing the simulation results with experiments, we suggest that the multiphonon relaxation channel is efficient at high temperature, while the Auger-type process may dominate the relaxation at low temperature. This combined mechanism can explain the weak temperature dependence at low temperature and stronger temperature dependence at higher temperature.

DOI: 10.1103/PhysRevB.79.235306 PACS number(s): 78.67.−n, 31.15.A−

I. INTRODUCTION

Nanocrystals (NCs) have attracted much attention during the last few decades due to their important applications in solar cells, lasers, thermoelectrics, etc.[1–3] These artificial molecules can be controlled in size, shape, topology, dopant, and surface passivation, providing large flexibility for achieving tailored properties. One hypothesis about semiconductor NCs is the phonon bottleneck effect[4] in which the discrete energy levels in NCs make it more difficult for phonons to match the electronic-energy gaps, and the cooling rate of hot carriers will significantly slow down. The phonon bottleneck effect has significant practical implications because the excess energy of the hot carriers may be extracted and utilized rather than losing to phonons so that the efficiency of the solar energy conversion may be greatly enhanced. Slowed electron relaxation in quantum dots has been observed in many experiments.[5–7] However, many other recent experiments have reported that the relaxation time is still fast (in the picosecond range) in InAs,[8] CdSe,[9] and PbSe (Refs. 10–12) nanocrystals and hence the phonon bottleneck effect is absent. Also, smaller NCs which have sparser energy levels than larger NCs were observed to relax more quickly than larger NCs.[10,13]

Various theories and models have been developed to interpret the observed slow or fast relaxation observed in these experiments. The slowed relaxation has been explained generally through the multiphonon relaxation mechanism. The fast relaxation in CdSe NCs has been successfully explained by considering other parallel relaxation channels such as the confinement-enhanced Auger-type process,[14–16] in which the electron unidirectionally transfers the energy to the hole, then the hole loses energy within subpicosecond via a fast relaxation process. The fast hole relaxation has been confirmed by experiments,[17] and the proposed relaxation mechanisms include multiphonon relaxation and a surface ligand-induced nonadiabatic (NA) relaxation channel.[18] Compared to CdSe, understanding of the fast relaxation in PbSe NCs is less clear because the Auger-type process was believed to be inefficient in PbSe. This is due to the mirrorlike symmetry in its electron and hole energy levels predicted by the effective-mass theory. However, recent empirical pseudopotential calculations showed that in PbSe the energy levels for holes are significantly denser than electrons,[19] so that the Auger-type process is still efficient[15] and can be the cause for the fast electron relaxation. More studies in the electronic structure of PbSe NCs are necessary to better understand this issue, which is part of the motivation of this work.

As pointed out in Refs. 17 and 18, the variation in the existing experimental observations and theoretical explanations indicates that parallel channels (including electron-phonon relaxation, Auger-type process, etc.) coexist in the relaxation process and their respective importance depends on the specific sample and surface conditions. Therefore, it is generally difficult to identify and decouple the relaxation channels from the experimental data. We notice that temperature dependence is a good qualifier to examine the relative importance of these relaxation channels. In all processes involving phonons, such as multiphonon relaxation and ligand-induced nonadiabatic relaxation, the temperature dependence should be strong. In contrast, the electron-hole energy transfer should not show a strong temperature dependence. The temperature dependence of carrier relaxation has been investigated in several experiments. Schaller *et al.*[10] observed that PbSe NC relaxation rates were temperature dependent while those of CdSe NC were not. Menzel *et al.*[8] showed temperature-activated relaxation in InAs/GaAs NC. Guyot-Sionnest *et al.*[20] showed that temperature will slightly decrease the relaxation rate in CdSe NC. The different temperature dependences for different NCs suggest that phonons play an important role in some NCs but not in others. Efforts were also devoted to theoretical investigations. For example, the empirical pseudopotential calculation by An *et al.*[15] shows that the PbSe relaxation rate increases with temperature in larger NCs and decreases in smaller NCs. This is not

fully consistent with the experimental results, mainly because the calculation is based on static lattice and the temperature effect can hardly be extracted. Thus, a time-domain study of the temperature-dependent relaxation rate is necessary to provide a deeper understanding of the carrier dynamics in semiconductor NC.

In this paper, an *ab initio* time-domain study of carrier relaxation rates is presented for PbSe NCs. To analyze the roles of electron, hole, and phonon in the decay process, the electronic density of states (DOS) is first calculated. Then the electron-phonon coupling spectrum is investigated by a Fourier transform of the evolution of the electronic and hole energy levels. The NA molecular dynamics (MD) is applied at different temperatures for the PbSe NC and the relaxation rates are evaluated. The temperature-dependent relaxation rates are analyzed and compared with experimental and theoretical results.

II. THEORY AND SIMULATION DETAILS

The real-time *ab initio* simulation of hot-carrier dynamics is carried out by the implementation of trajectory surface hopping (TSH) (Refs. 21 and 22) within time-dependent (TD) Kohn-Sham (KS) theory. Detailed theory can be found in Ref. 23. Only some key equations are shown here.

The single-particle KS equation is

$$i\hbar\frac{\partial\varphi_p(x,t)}{\partial t} = H\varphi_p(x,t), \quad p = 1, \ldots, N_e, \tag{1}$$

where the N_e is the number of electrons, $\varphi_p(x,t)$ are single electron KS orbitals, and H is the Hamiltonian which depends on the KS orbitals. In the density-functional theory (DFT), the Hamiltonian consists of the kinetic energy, electron-ion interaction, electron-electron Coulomb interaction, and exchange and correlation potential. We expand the time-dependent $\varphi(x,t)$ in the adiabatic KS orbitals $\tilde{\varphi}_p(x;R)$,

$$\varphi_p(x,t) = \sum_k^{N_e} c_{pk}(t)|\tilde{\varphi}_k(x;\mathbf{R})\rangle, \tag{2}$$

where $\mathbf{R}$ is the ion configuration. The TDDFT [Eq. (1)] then becomes an equation of motion of the coefficients

$$i\hbar\frac{\partial c_{pk}(t)}{\partial t} = \sum_m^{N_e} c_{pm}(t)(\epsilon_m\delta_{km} + \mathbf{d}_{km}\cdot\dot{\mathbf{R}}). \tag{3}$$

The NA coupling is given by

$$\begin{aligned}\mathrm{NA} = \mathbf{d}_{km}\cdot\dot{\mathbf{R}} &= -i\hbar\langle\tilde{\varphi}_k(x;\mathbf{R})|\nabla_{\mathbf{R}}|\tilde{\varphi}_m(x;\mathbf{R})\rangle\cdot\dot{\mathbf{R}} \\ &= -i\hbar\langle\tilde{\varphi}_k|\frac{\partial}{\partial t}|\tilde{\varphi}_m\rangle.\end{aligned} \tag{4}$$

Here d is the electron-phonon coupling term defined by $\langle\tilde{\varphi}_k(x;\mathbf{R})|\nabla_{\mathbf{R}}|\tilde{\varphi}_m(x;\mathbf{R})\rangle$. The NA coupling is determined by the adiabatic KS orbitals on the ion trajectory and can be calculated using right-hand side of Eq. (4).

TSH describes the electron hopping between electronic-energy levels. The probability depends on the ionic evolution. In fewest switches TSHs, the hopping probability between states k and m within time interval dt is

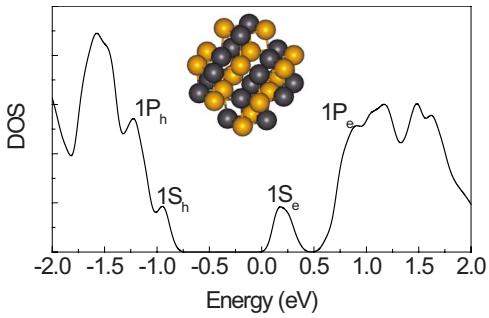

FIG. 1. (Color online) The average DOS during a 4 ps trajectory of the 32-atom NC. The average temperature is around 300 K.

$$dP_{km} = \frac{b_{km}}{a_{kk}}dt, \tag{5}$$

where

$$b_{km} = -2\,\mathrm{Re}(a_{km}^*\mathbf{d}_{km}\cdot\dot{\mathbf{R}}), \quad a_{km} = c_k c_m^*. \tag{6}$$

Here, c_k and c_m are the coefficients evolving according to Eq. (3). From the above equations, the real-time population of each electronic orbital is determined.

The TSH theory is implemented with the VASP package.[24] The Perdew-Wang exchange and correlation functional[25] and Vanderbilt pseudopotential[26] are used for the calculation. Only Γ point calculation is necessary for NCs. "Low" and "accurate" precisions within VASP are used for the MD and wave-function calculations, respectively, corresponding to plane-wave cutoff values of 116.381 and 155.175 eV. The initial structure of the 32-atom spherical PbSe NC ($Pb_{16}Se_{16}$) is cut from a bulk PbSe which has a rocksalt lattice structure. The diameter of this NC is approximately 1 nm. Unlike CdSe NCs,[27,28] PbSe is strongly ionic and the electronic properties are not much influenced by the surface structure,[29,30] thus the surface is not passivated.

Using the *ab initio* MD capability of VASP, the system is brought to different temperatures, and then a 4 ps microcanonical trajectory is generated for each temperature. An ionic step of 1 fs is used for the MD process, while an electronic step of 10^{-3} fs is used for electronic transitions. The MD step is significantly longer than the electronic step since the atoms are much heavier than electrons and move much more slowly. The initial conditions for the TSH are sampled from the trajectory. The initial electron-hole excitation is chosen as the most optically active electronic transition within a certain energy range. This energy range is chosen as 1.2–1.6 eV above the lowest unoccupied molecular orbital (LUMO) for electrons or below the highest occupied molecular orbital (HOMO) for holes.

III. RESULTS

A. Electronic structure and optical spectra

The average electronic DOS during an MD run at around 300 K is shown in Fig. 1. Although our NC is smaller comparing with experiments, the *S* and *P* peaks for electrons and

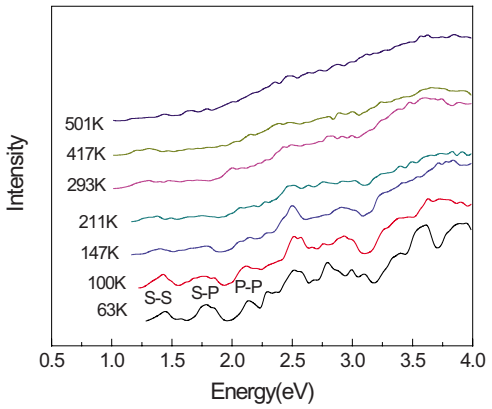

FIG. 2. (Color online) The absorption spectra of the 32-atom NC at different temperatures. The curves shown are the average value during a 4 ps microcanonical MD run. The higher temperature curves are shifted upward for comparison.

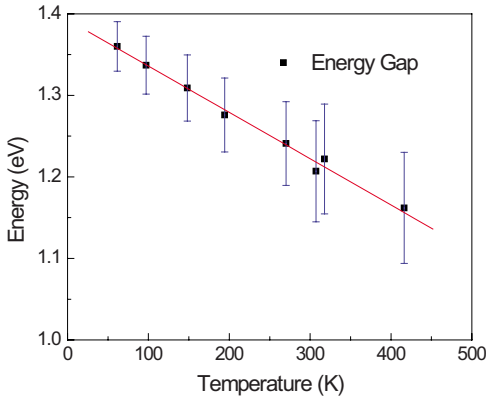

FIG. 3. (Color online) The average electronic band gap during an MD run. The bars show the standard deviations.

holes can still be observed, as marked in Fig. 1. From the atomistic point of view, the DOS peaks are actually concentrated electronic-energy levels, which correspond to single electron and hole states in effective-mass approximation (EMA).[31] It is clear that the hole states are denser than the electron states, a fact which disproves the mirrorlike symmetric electron and hole states predicted by EMA or tight-binding model.[32] The asymmetric electron and hole states are also seen in other pseudopotential based calculations.[19] This contradiction lies in that EMA assumes $m_e \approx m_h$ at L point of the Brillouin zone of PbSe, but in NCs where the Brillouin zone collapses to a single point, Σ point also contributes to the hole states.[19] The energy separation between $1S_h$ and $1S_e$ states in our calculation (also known as the band gap) is around 1.2 eV, which is smaller than the experimental value. Schaller *et al.*[10] obtained 1.8 eV band gap for PbSe NC with a diameter of 2.8 nm. A smaller NC should have an even larger electronic band gap. The underestimation of the band gap is normal for generalized gradient approximation (GGA) calculations.[33]

The calculated temperature-dependent optical-absorption spectra are shown in Fig. 2. These spectra contain the transitions across the electronic band gap, i.e., transitions from the valence band (VB) to the conduction band (CB). Based on the calculated electronic DOS in Fig. 1, the transition energies between the DOS peaks are around 1.2 eV ($1S_e1S_h$), 1.5 eV ($1S_e1P_h$), 1.7 eV ($1P_e1S_h$), and 2.1 eV ($1P_e1P_h$). Thus the first three peaks can be identified as the $1S_e1S_h$, nearly degenerate $1S_e1P_h$ and $1P_e1S_h$, and $1P_e1P_h$ transitions. The $1P$ to $1S$ transition is symmetry forbidden based on EMA. However, it is shown here that the asymmetry of the electronic DOS allows this transition to happen. The $1P1S$ peak is relatively strong in our calculation. This is partly due to the small size of our NC in which the asymmetric effect of wave functions is amplified.

As seen in Fig. 2, the peaks are broadened at higher temperatures. This is because phonon occupation number increases with temperature and more phonons couple to the photon-absorption process. Also seen is that the peaks shift to lower energy at higher temperature. The temperature-dependent $1S$ peak energy, known as the electronic band gap, is shown in Fig. 3. The plotted band-gap values are obtained by averaging the band-gap value during MD. The error bars are the standard deviations of the band-gap values. Our calculation shows consistency with former experiments and calculations. For PbSe NC with a diameter smaller than 4 nm, negative dE_g/dT is observed in the experiment[34] and also confirmed by pseudopotential calculations.[35] The smaller band gap and larger deviations at higher temperature can be attributed to the thermal expansion of the lattice and the temperature-dependent electron-phonon coupling.[36]

B. Electron-phonon coupling

The electron-phonon coupling is directly related to the second derivative of the energy along the nuclear trajectory, and therefore those vibrational modes that most strongly modulate the energy levels create the largest coupling.[23] Figure 4 shows the evolution of LUMO and HOMO and their Fourier transforms at 63 and 501 K. The oscillation amplitude of energy levels is evidently larger at high temperature. In both LUMO and HOMO cases, we see some evident coupling peaks at frequencies higher than 150 cm^{-1}, while the zone-center (Γ point) transverse and longitudinal optical-phonon frequencies for bulk PbSe are only 44 and 133 cm^{-1}, respectively.[37] These new high-frequency phonon modes are probably introduced on the surface of the NC due to the surface shrinking effects.[38]

From Fig. 4 we see that both carriers at all temperatures couple more strongly to lower frequency modes, which is consistent with the coherent-phonon measurements.[39,40] Unlike the carrier relaxation dynamics in bulk semiconductor where only high-frequency optical phonons are important, we find that in the NC, acoustic modes are also largely involved.[41] It can be seen from Fig. 4 that the temperature affects the coupling in two ways. First, at higher temperature, the Fourier transforms show a high-frequency tail, indicating that a larger fraction of high-frequency surface modes are involved in the carrier decay dynamics. This can be understood by considering that increased temperature can activate higher-frequency modes. Second, the Fourier transform curves at higher temperature are broadened, indicating that more modes are modulating the energy levels. This is be-

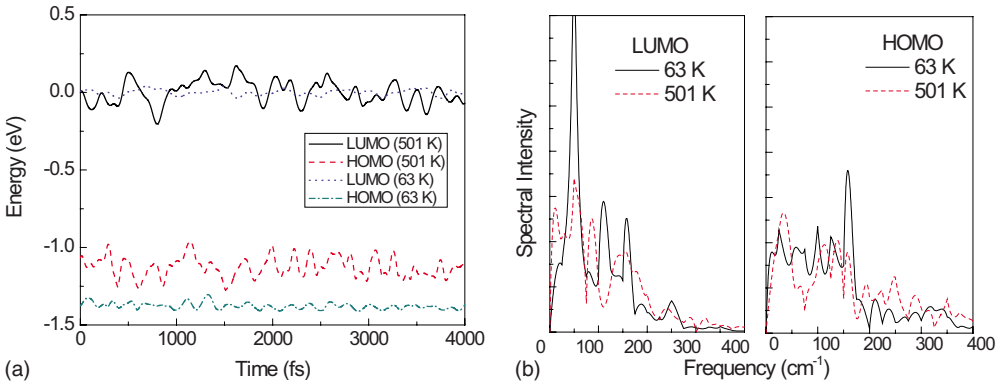

FIG. 4. (Color online) The time-resolved evolutions of LUMO and HOMO and their Fourier transforms at 63 and 501 K.

cause the anharmonic effect is stronger at a higher temperature.

C. Phonon-assisted decay

To study the hot-carrier decay process, the most optical active state between 1.2 and 1.6 eV above the LUMO (or below the HOMO) is chosen and populated for each trajectory. The decay will be driven by the perturbation of the electronic density due to the lattice vibrations. Lower energy levels will be gradually populated during the NAMD trajectories. The electronic energy averaged over the NAMD runs is shown in Fig. 5, which characterizes the decay process. The hole decays are faster but similar in shape, which are not shown here. The decay curve contains a Gaussian and an exponential component, similar to the previous calculations.[23,42] We find that the electronic energies at the end of the 3.5 ps trajectory are nearly zero at temperature higher than about 200 K, indicating that almost all electrons have decayed to the LUMO. The relaxation times for different temperatures are all in the picosecond range, which agrees well with experiments. Also the electronic relaxation time is longer at low temperature, confirming the fact that the phonon-assisted hot-electron decay is temperature activated.

To avoid ambiguity, we simply define the relaxation time as the time when the electronic or hole energy decays to $1/e$ toward average LUMO (for electron) or HOMO (for hole).

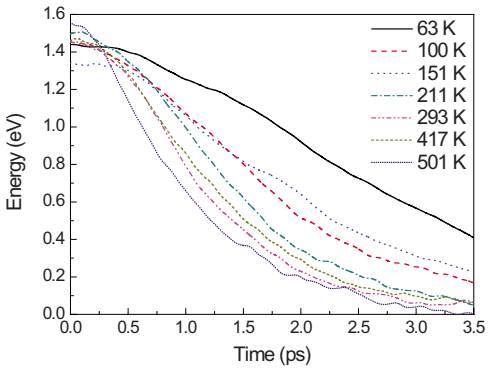

FIG. 5. (Color online) The average electron energy decay for different temperatures during a 3.5 ps trajectory. Zero energy is set as the average energy of LUMO.

Based on this definition, the carrier relaxation times at different temperatures are evaluated and compared with the experiments, as shown in Fig. 6. Here we see that the electron decay is much slower than the hole decay, which can be explained by the denser hole states, as rationalized below. The NA coupling defined in Eq. (4) can be rewritten as[43]

$$\mathrm{NA} = -i\hbar \frac{\langle \tilde{\varphi}_k | \nabla_{\mathbf{R}} H | \tilde{\varphi}_m \rangle}{E_m - E_k} \cdot \dot{\mathbf{R}}, \tag{7}$$

indicating that its strength is inversely proportional to the difference between the energy levels ΔE. Based on the time-dependent perturbation theory, the transition rate is proportional to $|\mathrm{NA}|^2$, so the decay rate for an energy difference of ΔE is proportional to $1/(\Delta E)^2$. Thus, the denser hole states ensure the hole to relax more quickly than the electron.

Both electron and hole relaxations show temperature activation. This can be easily understood since more phonons are excited at higher temperature and the carrier-phonon scattering should be more frequent. However, to our knowledge, no quantitative model has been developed on the temperature dependence of hot-carrier decay in the NC. Here we present a simple model based on our formalism in Sec. II. Notice that from Eq. (4), if we assume d_{km} is only implicitly

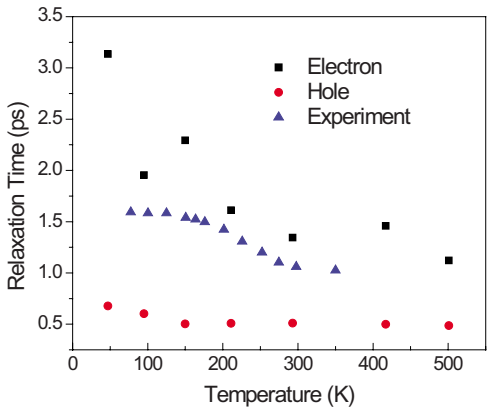

FIG. 6. (Color online) The calculated electron and hole relaxation times at different temperatures. Also shown is the temperature-dependent hot-carrier relaxation time for NC with an average diameter of 3.8 nm.

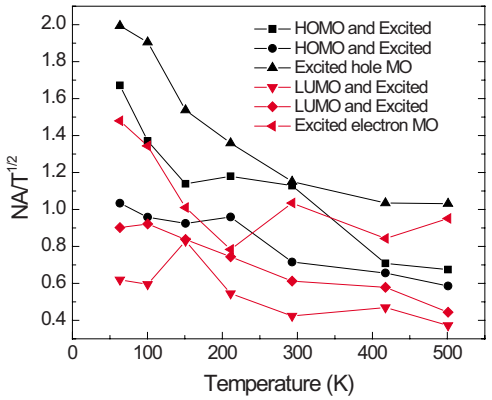

FIG. 7. (Color online) The temperature-dependent coupling strength of electron and hole.

dependent on temperature, the NA coupling strength is proportional to the ion velocities $\dot{\mathbf{R}}$, in turn to the square root of the kinetic energy E_k,

$$\mathrm{NA} \sim \sqrt{E_k}. \tag{8}$$

Because the MD process treats the ions classically, MD temperature T_{MD} is related to E_k of the system by a simple equation

$$3Nk_BT_{\mathrm{MD}} = 2E_k, \tag{9}$$

where N is the number of particles in the system and k_B is the Boltzmann constant. From the time-dependent perturbation theory, a simple estimation is that the transition probability is proportional to the square of the off-diagonal element of the perturbation matrix, which is $|\mathrm{NA}|^2$ in our case. Based on the above considerations, the temperature dependences of the relaxation time and rate are expected to be

$$\tau \sim \frac{1}{T_{\mathrm{MD}}}, \quad \gamma \sim T_{\mathrm{MD}}. \tag{10}$$

Our calculated results deviate from this trend. Both electron and hole decay times can be better fitted to $T^{-0.4}$ than T^{-1}. The weaker temperature dependence can only be attributed to the temperature dependence of electron-phonon coupling strength, i.e., the d_{km} term in Eq. (4). To investigate this term, we randomly choose four excited energy levels for the electrons and calculate the NA coupling strength between pairs of these levels or between one of these levels and LUMO. Similar calculations are carried out for the holes. To rule out the explicit temperature-dependent term $(\dot{\mathbf{R}})$ and leave only the d term, we show the dependence of $\mathrm{NA}/\sqrt{T}$ on the temperature, as in Fig. 7. As expected, they decrease as the temperature increases. The temperature dependence can be well fitted to the form $T^{-0.3}$. Therefore, the whole NA coupling term has a temperature dependence of $T^{0.2}$. Thus the weaker $T^{-0.4}$ dependence of relaxation time on temperature can be explained simply considering $\tau \sim |\mathrm{NA}|^{-2}$. The temperature dependence of the d term is most likely due to the dilation of the NC at high temperature. Although the thermal expansion is weakly dependent on temperature, the coupling term has a rather strong dependence on the expansion. To understand this, we can simply consider the case of an infinite potential well: if the width of the potential well is a, the coupling term defined by $\langle m|\frac{d}{da}|n\rangle$ is proportional to a^{-2}.[44] This dependence is fairly strong and could explain the temperature dependence of the d term observed in Fig. 7.

IV. DISCUSSION

In general, the relaxation mechanism being discussed can be attributed to the interaction among electron, hole, photon, and phonon. Whatever the mechanism is, the energy acquired by absorption the photon, if not extracted by other ways, will finally dissipate to the lattice. Even the ligand-induced nonadiabatic relaxation proposed by Cooney *et al.*[18] can be viewed as a hole-phonon process. The difference of their relaxation mechanism is that the phonons may come from surface ligands' vibrations rather than the intrinsic NC vibrations. Three time scales are involved in the decay process, i.e., the electron-phonon decay time τ_1, the hole-phonon decay time τ_2, and the electron-hole energy-transfer time τ_3. The multiphonon process and the Auger-hole process (here it means Auger-type electron-hole energy transfer and hole-phonon process) are parallel channels,

$$\tau = 1/\left(\frac{1}{\tau_1} + \frac{1}{\tau_2 + \tau_3}\right). \tag{11}$$

There has been debating about the relative importance of these two relaxation channels. As we see in the theoretical calculation and experiments, τ_1, τ_2, τ_3 are all in the subpicosecond and picosecond ranges. The first two should have a strong dependence on temperature while the last one should not. The overall temperature dependence is determined by which channel is more efficient.

Our electron-phonon decay rate has a much stronger temperature dependence than experimental result, especially at low temperatures, indicating that multiphonon decay process is not efficient at low temperature. Based on our calculations, both the electron-phonon decay and Auger-hole decay should be temperature dependent but the hole decay is relatively fast, thus the temperature dependence of the Auger hole is less evident. In the case of PbSe, we believe that the Auger channel at low temperature is more efficient than the multiphonon channel, which gives the weak temperature dependence. At higher temperature, when the electron-phonon channel becomes more efficient, it will contribute to the overall relaxation rate and then stronger temperature dependence is observed. This scenario explains the weak temperature dependence of relaxation time at low temperature and the relatively stronger temperature dependence at higher temperature.

This explanation also works for CdSe, for which the relaxation is observed to be almost temperature independent.[10] In the case of CdSe, where the hole is much heavier than electron, the hole decay time will be much shorter than electron. We expect that the temperature dependence for hole relaxation in CdSe will be even weaker than in PbSe because the CdSe hole states are even denser. Thus the Auger-hole channel will dominate over electron-phonon decay in the de-

cay process even at very high temperature. The temperature dependence of the electron relaxation which then comes from the hole-phonon decay can be too weak to be observed by the existing experiments. This explains why a temperature dependence is not seen in the CdSe NC.

V. SUMMARY

We have investigated the phonon-assisted carrier relaxation rate in PbSe NC using a real-time *ab initio* method. Electronic structure and optical-absorption spectra are calculated first. The electronic structure shows the *S* and *P* peaks as predicted by the EMA. The DOS does not show a mirror-like symmetry across the band gap and the hole states are denser than the electron states. Temperature-dependent absorption spectra show that dE_g/dt in small PbSe NC is negative, different from bulk PbSe. The Fourier transforms of the LUMO and HOMO show that both acoustic phonon and optical phonon participate in the decay. At higher temperatures, more phonon modes couple to the electronic-energy levels because of the anharmonic effect.

Our calculated temperature-dependent relaxation time shows that both electron and hole relaxation times are in the picosecond scale and the relaxation is temperature activated. The temperature dependence of the relaxation time can be described by $1/T_{\mathrm{MD}}^{0.4}$. The electron relaxes more slowly than hole and the temperature dependence of hole relaxation is less evident than electron. The experimentally observed temperature dependence of the relaxation in PbSe is explained by considering both multiphonon and Auger-hole relaxation channels: at low temperature the Auger-hole relaxation dominates, while at higher temperature the multiphonon relaxation becomes more efficient.

ACKNOWLEDGMENTS

This work was supported by a faculty startup fund from Purdue University. O.V.P. acknowledges support from DOE under Grant No. DE-FG02-05ER15755 and ACS PRF under Grant No. 41436-AC6.

*Author to whom correspondence should be addressed.
†prezhdo@chem.washington.edu
‡ruan@purdue.edu

[1] V. I. Klimov, J. Phys. Chem. B **110**, 16827 (2006).
[2] J. Urayama, T. B. Norris, J. Singh, and P. Bhattacharya, Phys. Rev. Lett. **86**, 4930 (2001).
[3] M. S. Dresselhaus, G. Chen, M. Y. Tang, R. G. Yang, H. Lee, D. Z. Wang, Z. F. Ren, J. P. Fleurial, and P. Gogna, Adv. Mater. (Weinheim, Ger.) **19**, 1043 (2007).
[4] A. Nozik, Annu. Rev. Phys. Chem. **52**, 193 (2001).
[5] P. Guyot-Sionnest, M. Shim, C. Matranga, and M. Hines, Phys. Rev. B **60**, R2181 (1999).
[6] R. Heitz, A. Kalburge, Q. Xie, M. Grundmann, P. Chen, A. Hoffmann, A. Madhukar, and D. Bimberg, Phys. Rev. B **57**, 9050 (1998).
[7] A. Pandey and P. Guyot-Sionnest, Science **322**, 929 (2008).
[8] S. Menzel, E. A. Zibik, P. Aivaliotis, J. W. Cockburn, L. R. Wilson, and M. J. Steer, Phys. Rev. B **77**, 153302 (2008).
[9] M. B. Mohamed, C. Burda, and M. A. El-Sayed, Nano Lett. **1**, 589 (2001).
[10] R. D. Schaller, J. M. Pietryga, S. V. Goupalov, M. A. Petruska, S. A. Ivanov, and V. I. Klimov, Phys. Rev. Lett. **95**, 196401 (2005).
[11] J. M. Harbold, H. Du, T. D. Krauss, K. S. Cho, C. B. Murray, and F. W. Wise, Phys. Rev. B **72**, 195312 (2005).
[12] C. Bonati, A. Cannizzo, D. Tonti, A. Tortschanoff, F. van Mourik, and M. Chergui, Phys. Rev. B **76**, 033304 (2007).
[13] V. I. Klimov and D. W. McBranch, Phys. Rev. Lett. **80**, 4028 (1998).
[14] E. Hendry, M. Koeberg, F. Wang, H. Zhang, C. de Mello Donegà, D. Vanmaekelbergh, and M. Bonn, Phys. Rev. Lett. **96**, 057408 (2006).
[15] J. M. An, M. Califano, A. Franceschetti, and A. Zunger, J. Chem. Phys. **128**, 164720 (2008).
[16] P. Yu, J. M. Nedeljkovic, P. A. Ahrenkiel, R. J. Ellingson, and A. J. Nozik, Nano Lett. **4**, 1089 (2004).
[17] R. R. Cooney, S. L. Sewall, K. E. H. Anderson, E. A. Dias, and P. Kambhampati, Phys. Rev. Lett. **98**, 177403 (2007).
[18] R. R. Cooney, S. L. Sewall, E. A. Dias, D. M. Sagar, K. E. H. Anderson, and P. Kambhampati, Phys. Rev. B **75**, 245311 (2007).
[19] J. M. An, A. Franceschetti, and A. Zunger, Nano Lett. **6**, 2728 (2006).
[20] P. Guyot-Sionnest, B. Wehrenberg, and D. Yu, J. Chem. Phys. **123**, 074709 (2005).
[21] J. C. Tully, J. Chem. Phys. **93**, 1061 (1990).
[22] C. F. Craig, W. R. Duncan, and O. V. Prezhdo, Phys. Rev. Lett. **95**, 163001 (2005).
[23] S. V. Kilina, C. F. Craig, D. S. Kilin, and O. V. Prezhdo, J. Phys. Chem. C **111**, 4871 (2007).
[24] G. Kresse and J. Furthmuller, Comput. Mater. Sci. **6**, 15 (1996).
[25] J. P. Perdew and Y. Wang, Phys. Rev. B **45**, 13244 (1992).
[26] D. Vanderbilt, Phys. Rev. B **41**, 7892 (1990).
[27] A. Puzder, A. J. Williamson, N. Zaitseva, and G. Galli, Nano Lett. **4**, 2361 (2004).
[28] A. Puzder, A. J. Williamson, F. Gygi, and G. Galli, Phys. Rev. Lett. **92**, 217401 (2004).
[29] F. W. Wise, Acc. Chem. Res. **33**, 773 (2000).
[30] A. Franceschetti, Phys. Rev. B **78**, 075418 (2008).
[31] O. V. Prezhdo, Chem. Phys. Lett. **460**, 1 (2008).
[32] G. Allan and C. Delerue, Phys. Rev. B **70**, 245321 (2004).
[33] O. Pulci, G. Onida, R. Del Sole, and L. Reining, Phys. Rev. Lett. **81**, 5374 (1998).
[34] A. Olkhovets, R. C. Hsu, A. Lipovskii, and F. W. Wise, Phys. Rev. Lett. **81**, 3539 (1998).
[35] H. Kamisaka, S. V. Kilina, K. Yamashita, and O. V. Prezhdo, J. Phys. Chem. C **112**, 7800 (2008).
[36] T. J. Liptay and R. J. Ram, Appl. Phys. Lett. **89**, 223132 (2006).
[37] R. N. Hall and J. H. Racette, J. Appl. Phys. **32**, 2078 (1961).
[38] H. Bao, X. L. Ruan, and M. Kaviany, Phys. Rev. B **78**, 125417

(2008).
[39] D. M. Sagar, R. R. Cooney, S. L. Sewall, E. A. Dias, M. M. Barsan, I. S. Butler, and P. Kambhampati, Phys. Rev. B **77**, 235321 (2008).
[40] T. D. Krauss and F. W. Wise, Phys. Rev. Lett. **79**, 5102 (1997).
[41] U. Woggon, H. Giessen, F. Gindele, O. Wind, B. Fluegel, and N. Peyghambarian, Phys. Rev. B **54**, 17681 (1996).
[42] B. F. Habenicht, C. F. Craig, and O. V. Prezhdo, Phys. Rev. Lett. **96**, 187401 (2006).
[43] S. T. Epstein, *Force Concept in Chemistry* (Van Nostrand Reinhold, New York, 1981).
[44] D. Griffiths, *Introduction to Quantum Mechanics* (Prentice-Hall, Upper Saddle River, NJ, 1995).